mining

MDPI

Article

Evaluation and Prediction of Blast-Induced Ground Vibrations: A Gaussian Process Regression (GPR) Approach

Yewuhalashet Fissha [1,*], Hajime Ikeda [1], Hisatoshi Toriya [1], Narihiro Owada [1], Tsuyoshi Adachi [1] and Youhei Kawamura [2]

1 Department of Geosciences, Geotechnology and Materials Engineering for Resources, Graduate School of International Resource Sciences, Akita University, Akita 010-8502, Japan
2 Faculty of Engineering, Division of Sustainable Resources, Hokkaido University, Kita 8, Nishi 5, Kita-Ku, Sapporo 060-8628, Japan
* Correspondence: d6521115@s.akita-u.ac.jp

Abstract: Ground vibration is one of the most hazardous outcomes of blasting. It has a negative impact both on the environment and the human population near to the blasting area. To evaluate the magnitude of blasting vibrations, it is important to consider PPV as a fundamental critical base parameter practice in terms of vibration velocity. This study aims to explore the application of different soft computing techniques, including a Gaussian process regression (GPR), decision tree (DT), and support vector regression (SVR), for the prediction of blast-induced ground vibration (PPV) in quarry mining. The three models were evaluated using classical mathematical evaluation metrics (R^2, RMSE, MSE, MAE). The result shows that the GPR model achieves an excellent prediction result; with R^2 = 0.94, RMSE = 0.0384, MSE = 0.0014, and MAE = 0.0265, it shows high accuracy in predicting PPV. The Shapley additive explanation (SHAP) results emphasize the importance of understanding the interactions between the various factors and their effects on the vibration assessment. The findings can inform the development of more sustainable and environmentally friendly models for predicting blasting vibrations. Using a GPR to simulate and predict blasting-induced ground vibrations is the study's main contribution. The GPR can capture complicated, non-linear correlations in data, making it ideal for blast-induced ground vibrations, which are dynamic and nonlinear. By using a Gaussian process regression, we can help companies and researchers improve the safety and efficiency in blast-induced ground vibration environments.

Keywords: PPV; blasting; vibration; machine learning; prediction; mining; GPR; SVM

check for updates

Citation: Fissha, Y.; Ikeda, H.; Toriya, H.; Owada, N.; Adachi, T.; Kawamura, Y. Evaluation and Prediction of Blast-Induced Ground Vibrations: A Gaussian Process Regression (GPR) Approach. *Mining* **2023**, *3*, 659–682. https://doi.org/10.3390/mining3040036

Academic Editor: Philipp Hartlieb

Received: 25 September 2023
Revised: 23 October 2023
Accepted: 25 October 2023
Published: 26 October 2023

1. Introduction

Blasting is a vital operation in industries such as mining, construction, and quarrying. It involves the use of chemical explosives to break down rocks and other hard materials for various purposes, including the extraction of minerals and the construction of infrastructure [1–5]. However, conventional blasting practices have significant environmental implications [6–8]. The explosions produce pollutants that contaminate the air and water bodies, and the noise and vibrations disturb local ecosystems and communities [9–11]. Furthermore, the resultant land disturbances can lead to a loss of biodiversity and disrupt the natural landscape. If left unchecked, these operations can wreak havoc in the environment and lead to unsustainable development patterns. Given growing environmental awareness and concerns, businesses and industries can no longer ignore the ecological footprint of their operations. Public and regulatory bodies demand greater responsibility and accountability from industries, especially those with significant environmental impacts such as blasting. Khandelwal et al. [12] described ground vibration because of an explosion in a rock mass during the blasting process. The blast hole explodes with a detonating charge that fractures the rock. Due to fast rock velocity following a blast hole explosion, significant dynamic stresses are created. As strain waves propagate through a rock mass, wave-like oscillations occur. The strain energy of these strain waves causes radial cracking, crushing, and reflection fractures in the free face of the bench. Permanent rock volume deformation results from fractured and radial fracture zones. Therefore, the ground vibration seen during an explosion is a result of the energy release, and its strength is affected by different factors, such as the amount of explosive material used, the specific rock composition subjected to blasting, and the proximity to the blast origin [13–17]. Several studies conducted by various researchers [17,18] have identified a relationship between the magnitude of ground vibrations caused by blasts and the controllable and uncontrolled parameters associated with the blasting procedures. The controllable variables associated with blasting include various blast design parameters, such as burden, spacing, blast hole depth, hole diameter, stemming type and height, maximum charge weight per delay (W), and specific charge. Additionally, explosive parameters, such as explosive type, detonation velocity (VoD), and powder factor, are also subject to modification and are carefully planned based on the existing conditions. Hence, the duty of adjusting and strategising these controllable blasting parameters during the design phase may lie with the blasting engineer. The uncontrolled variables include the mechanical and physical characteristics of the rock as well as the geological qualities of the surrounding environment. Most uncontrolled components are dependent on the rock's inherent formation.

Over the last few decades, different empirical formulas have been developed by different scholars to predict the magnitude of ground vibrations caused by blast-induced events. The first equation, developed by the United States Bureau of Mines (USBM) and Duvall Fogleson, is a major predictor of peak particle velocity (PPV). Throughout an extended period, several researchers have modified the USBM formula, including elements such as the scaled distance and maximum instantaneous charge (MIC). However, the process of predicting and evaluating blasting vibrations is more difficult and requires more time due to several aspects. These elements include accurate prediction models, input data parameters, evaluation of rock mass conditions, and consideration of additional criteria. Hence, it can be concluded that the empirical models are considered insufficient to predict the PPV due to the inherent limitations associated with the empirical formulas. To solve this problem, many researchers are considering utilising AI techniques for the prediction of blast-induced vibrations. Some of the research on blast-induced vibrations based on AI and machine learning are summarised in Table 1. This study utilised a blasting data sample to predict the PPV of dolomite quarry mining by employing different machine learning methods. Three machine learning methods were included in this study, a decision tree (DT), support vector machine (SVM), and Gaussian process regression (GPR), to achieve the study aims. The coefficient of determination (R^2), mean squared error (MSE), mean absolute error (MAE), and root-mean-squared error (RMSE) are used to compare the predicted and measured results. In addition, a Shapley additive explanation (SHAP) analysis was conducted to investigate the relationship between the input variables and the PPV. As a result, the information gathered can be used to run the machine learning methods, estimate the vibration induced from the blasting, and evaluate the influence of the input factors.

Table 1. Summary of previous study based on the prediction of PPV using AI and machine learning techniques.

Authors	Total Datasets	Input Parameters	AI Models	Evaluation Metrics
Armaghani et al. [19]	109	BS, MC, HD, ST, SD, DI, PF, RQD	ANFIS	R^2 = 0.97
Vasovic et al. [20]	32	D, TC, MCPD	Empirical predictor, ANN	R^2 = 0.9 RMSE = 0.018
Khandelwal and Singh [21]	150	B, S, MCPD, HD, D V, E, Pv, BI, VoD	ANN, MVRA, empirical model	MAE = 0.24

Table 1. *Cont.*

Authors	Total Datasets	Input Parameters	AI Models	Evaluation Metrics
Nguyen et al. [22]	136	DI, MC	HKM-CA	R^2 = 0.99
Saadat et al. [17]	69	D, MCPD, HD	ANN, MLR, empirical model	R^2 = 0.95 MSE = 0.00072
Lawal [23]	100	D, MCPD	ANN, MLR	R^2 = 0.988, RMSE = 2.90, VAF = 98.74 MAPE = 7.14
Zhang [24]	175	PF, T, B, S H, D, MCPD	PSO-XG Boost, empirical models	R^2 = 0.96 RMSE = 0.58, MAE = 0.34 VAF = 96.08
Rana et al. [25]	137	MCPD, HDM, CPH, HD, TC, D, NH, TS	ANN, MVRA, CART, empirical predictor	RMSE = 1.56 R^2 = 0.95
Verma and Singh [26]	127	MCPD, TC HD, B, S, T,	GA, ANN, MVRA, empirical predictor	R^2 = 0.99 MAPE = 0.088
Ghasemi et al. [27]	120	B, S, T, NH, MCPD, D	ANFIS-PSO, SVR	R^2 = 0.96 RMSE = 1.83
Iphar et al. [28]	44	MCPD, D	ANFIS, MLR	R^2 = 0.98 RMSE = 0.80

Research Significance

The issue of blast-induced ground vibrations has considerable significance across several industries, such as mining and construction, owing to their subsequent impact. Traditional models often rely on deterministic or empirical methodologies that can fail to sufficiently account for the complex interrelationships among the variables involved, leading to predictions that lack precision. The use of a Gaussian process regression (GPR) to analyse the vibrations introduces a unique methodology that is based on realistic data and can accurately represent the fundamental complexities and uncertainties associated with the phenomenon.

This study has twofold significance. The present study aims to fill a notable need in existing research by integrating robust machine learning techniques, namely a GPR, in the investigation of ground vibrations resulting from explosive occurrences. Furthermore, this study has significant practical implications, as the suggested model may be adapted to accommodate various blasting procedures and geological conditions. This versatility renders it a valuable tool for engineers, policymakers, and scholars to address the environmental and structural impacts of blasting activities.

2. Materials and Methods

2.1. Study Area

The Golden Girl dolomite quarry is found at Ikpeshi and its environs in Akoko Edo, Edo State, which lies within longitudes 6°10′ E to 6°15′ E and latitudes 7°08′ N to 7°10′ N and is one part of the Igarra schist belt, the Southwestern basement complex of Nigeria (see Figure 1). This is part of the largest lithology component that makes up the geology of Nigeria, and the basement rocks are made up of four major groups observed within this area, according to Taiwo [5]. These are the migmatite–gneiss complex, the metasediments (marble, schists, calc-silicate rock, quartzites), and the porphyritic older granite, which is discordant with the non-metamorphosed syenite dyke Taiwo [5]. The calc-silicate rocks are like marble and medium- to coarse-grained with peripheralists. In short, about 80% of the Akoko Edo area is underlain by carbonaceous rocks.

(**a**)

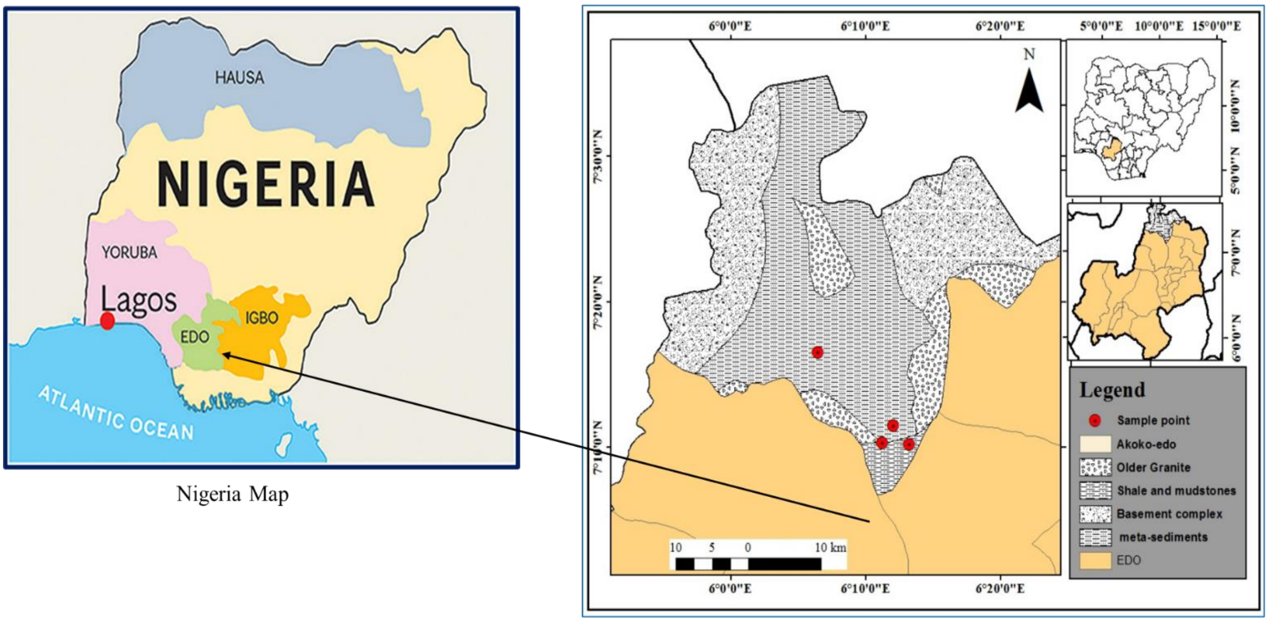

Nigeria Map

Akobo Edo Map

(**b**)

Figure 1. (**a**) Akobo Edo map and (**b**) dolomite quarry face.

2.2. Blasting Vibration Monitoring Procedures at the Quarry Site

The use of monitoring instruments is essential to accurately measure the vibrations resulting from quarry blasting activities. The first stage of installation involves identifying and placing all the monitoring equipment. Before proceeding to monitor the vibrations, the team of experts in the quarry assessed the dimensions of the quarry and the pit in general (see Figure 2), the technique used for blasting, and the proximity to surrounding buildings.

After establishing the ideal position, the equipment was installed and calibrated in accordance with the manufacturer's specified instructions. A variety of vibration-measuring devices were used at the quarry location and thereafter positioned in accordance with the pre-established arrangements. The main devices used in our investigation consisted of a laptop computer, vibration meter, geophone, and sensor recorder. Figure 3 depicts the comprehensive array of equipment used in the investigation. Data loggers are used for the purpose of acquiring and preserving data derived by seismographs, which may then be subjected to analyses and utilised to modify the blasting method to minimize the impact on the environment. Ensuring the safe and effective operation of quarries necessitates the use of proper technologies for monitoring blasting vibration.

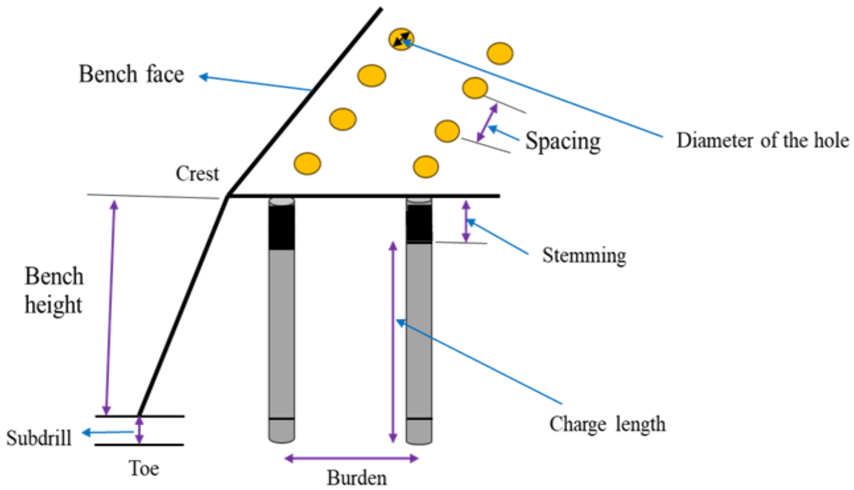

Figure 2. Structure of open-pit mining.

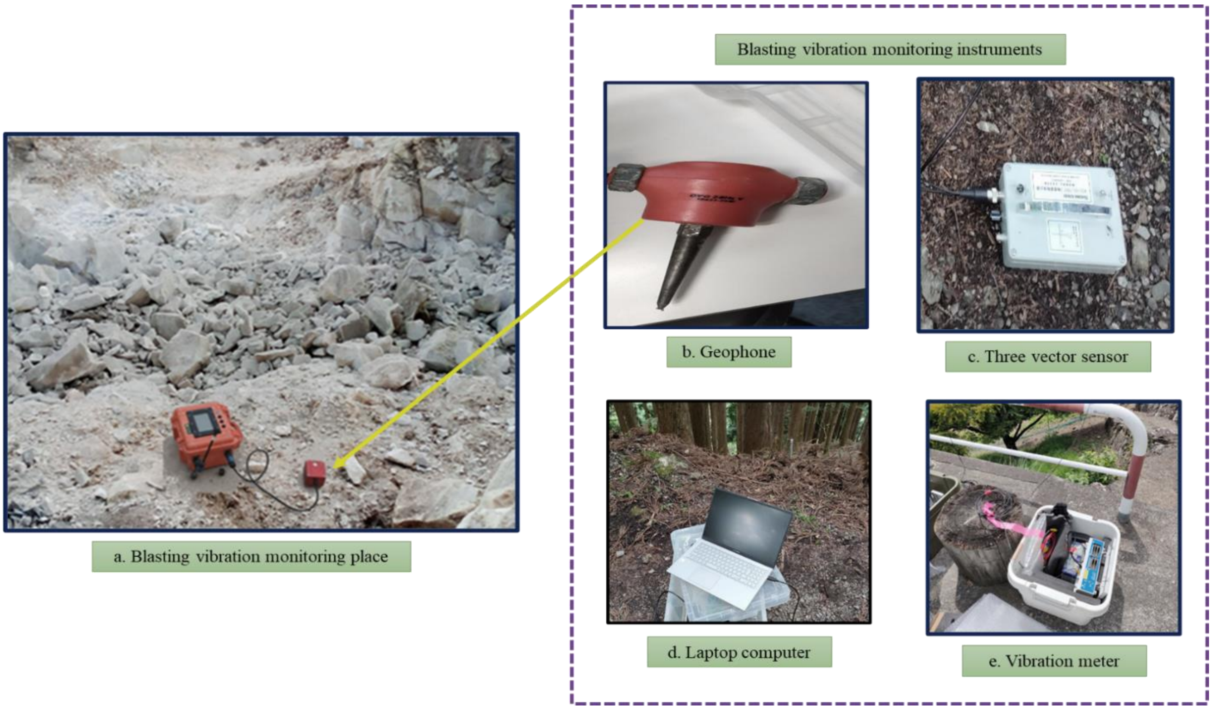

Figure 3. (**a**) Dolomite quarry mining with the blasting vibration monitoring place and the blasting vibration instruments. (**b**) Geophone, (**c**) three vector sensor, (**d**) Laptop computer, and (**e**) Vibration meter.

2.3. Data Analysis

To develop accurate models for predicting ground vibrations generated by blasting, the authors conducted an analysis using a dataset acquired from the Golden Girl dolomite quarry located in Akobo Edo State, Nigeria. The dataset consists of 140 instances of blasting data, including a range of possible input factors that were examined for their potential impact on the blasting ground vibrations, namely the PPV. In this study, we used Origin pro 2023b learning edition software to analyse and visualize the data statistically. The variables considered in this study include the number of blast holes (n), ratio of burden to hole diameter (B/De), ratio of bench height to burden (H/B), maximum instantaneous charge (Q), scaled distance (SD), spacing (S), and burden (B). Figure 4 shows the visual representation of the distribution of each variable (i.e., input and output) in the form of a histogram. The use of visual aids, such as the figure shown, proved to be significant for identifying any possible irregularities or patterns that may have an impact on the accuracy of the models.

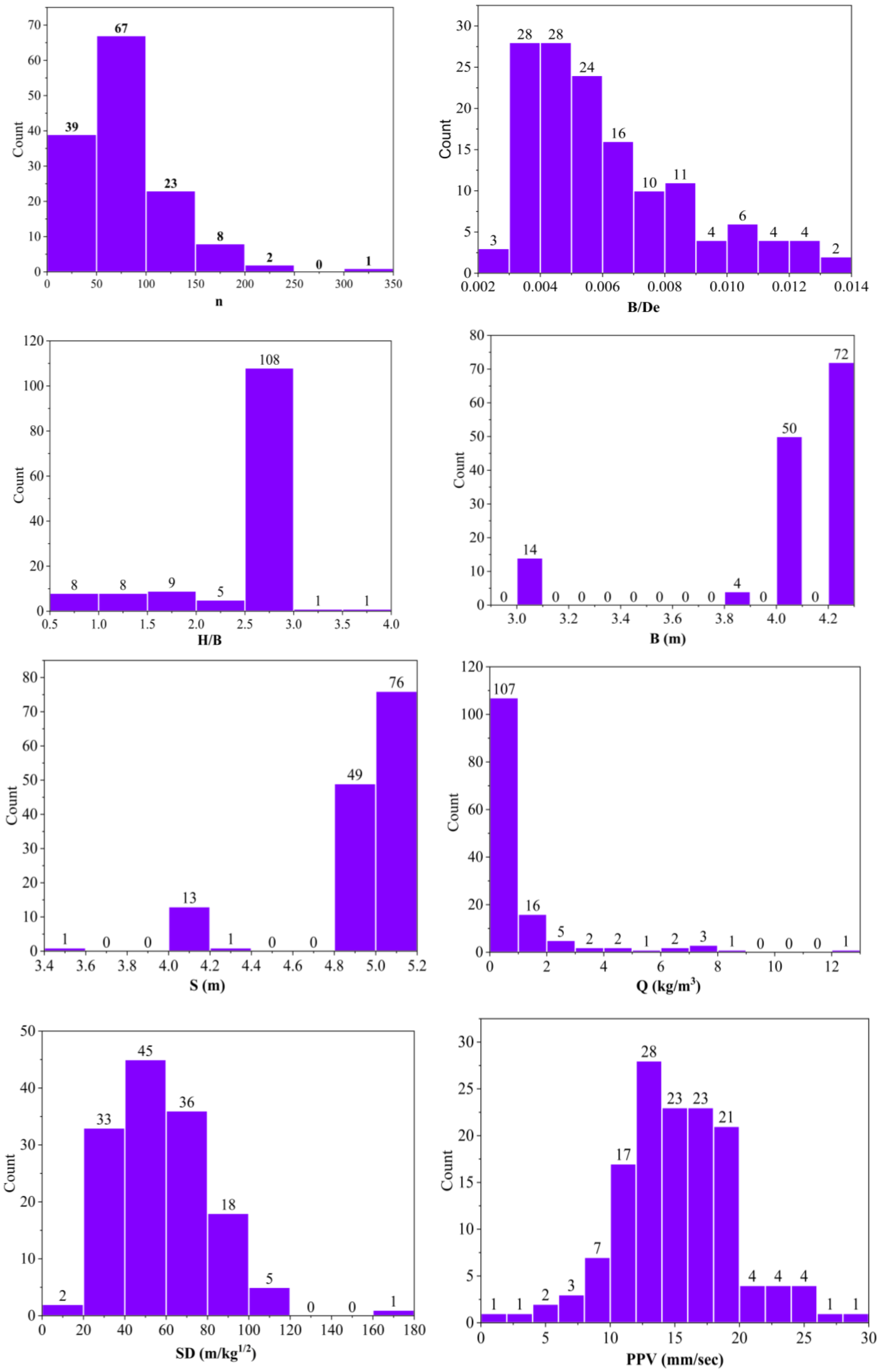

Figure 4. Distribution of the variables in the form of a frequency graph.

The Pearson correlation coefficient, which ranges from −1 to 1, is essential for assessing the correlation coefficient between two variables [29]. A correlation value of zero implies that there is no association between the variables, whereas a positive correlation coefficient suggests a positive relationship, and a negative correlation coefficient indicates a negative relationship.

Furthermore, the degree of correlation may be determined by examining the magnitude of the correlation coefficient, wherein a higher absolute value indicates a more robust connection between the variables. According to the data shown in Figure 5, a significant positive connection was seen between B and S, with value of 0.94. However, a negative correlation was observed between B/De, Q, SD, and PPV. It is vital to understand that the Pearson coefficient alone offers an understanding of the linear association between two variables only. However, for nonlinear relationships, the Pearson correlation is not convenient.

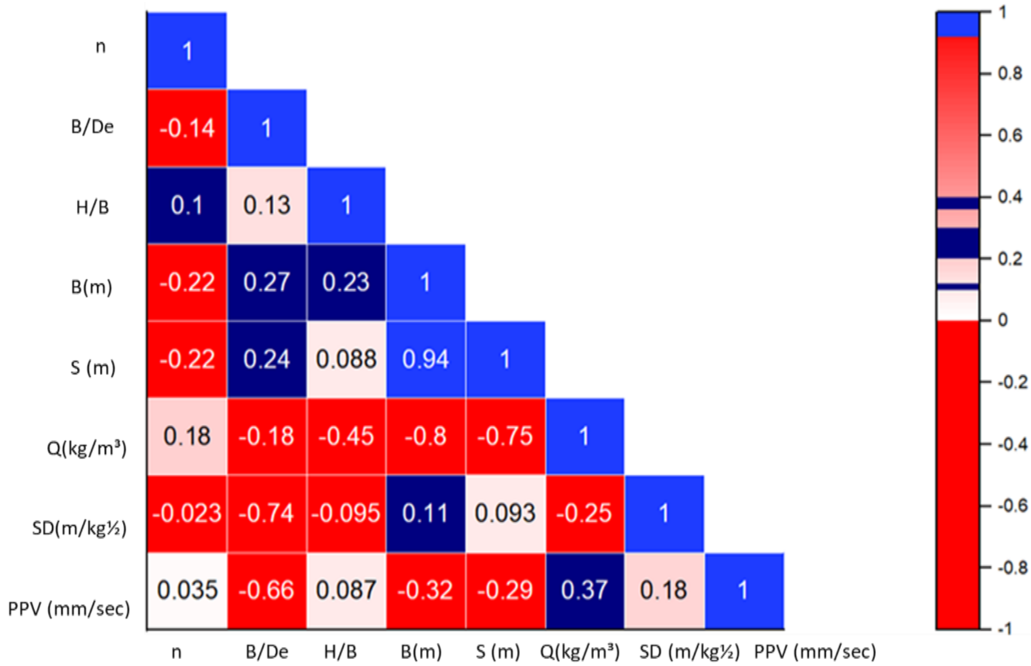

Figure 5. Pearson correlation graph for both input and output variables.

In this study, a Spearman correlation coefficient was used to obtain a nonlinear relationship between the variables. This method does not assume a linear relationship between variables. The Spearman correlation coefficient also ranges from −1 to 1, but it measures the strength of monotonic relationships (increasing or decreasing) rather than strictly linear relationships [30]. This makes the Spearman correlation suitable for capturing nonlinear and linear relationships. Unlike the Pearson correlation, it does not assume that the data are normally distributed or that the relationship is linear. In Figure 6, it can be observed that the variable n exhibits the highest values of interaction information for the variable PPV. This suggests that these two variables have a stronger relationship than that of other variables in the dataset.

Figure 7 depicts a visualisation of the data distribution using a violin box plot at the quartile ranges of 25% and 75%. Based on this, the PPV is found in a range of 7 to 15 mm/s.

According to the scope of this study, the use of a two-dimensional kernel density estimation (KDE) has shown significant utility in capturing the complex patterns contained in the blasting dataset. The KDE method allows for an efficient simultaneous evaluation of the density distribution of two continuous variables, such as each input variable and the output variable (PPV). This feature is especially beneficial when a traditional scatter plot can hide underlying patterns because of the excessive overlapping of data points. The use of a two-dimensional kernel density estimation (KDE) methodology enhances the visual representation of the results in this research. The density can be represented using colour gradients, as shown in Figure 8.

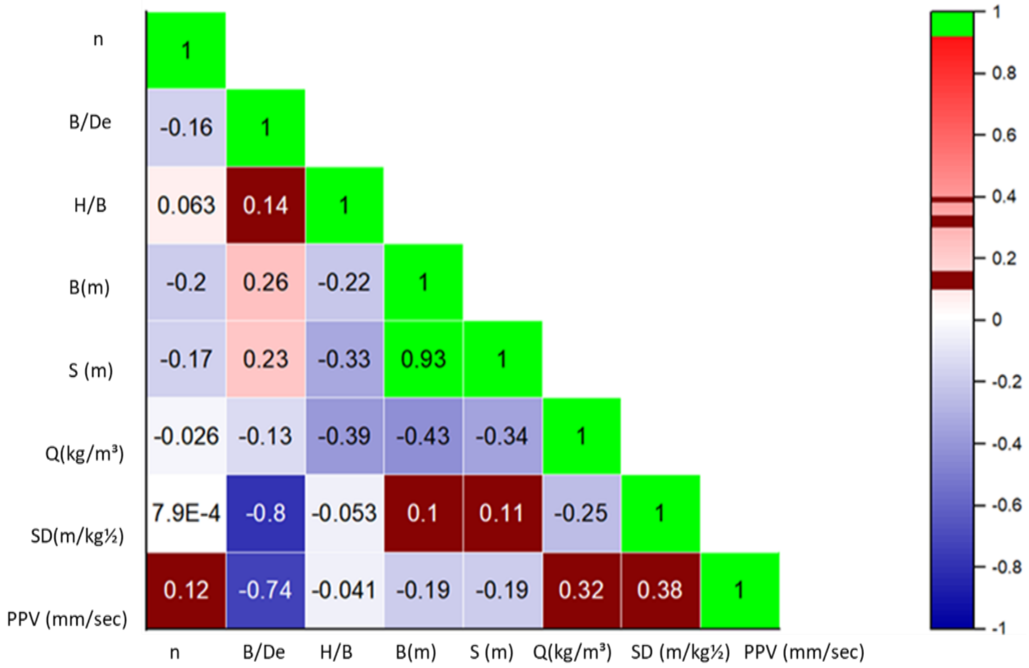

Figure 6. Spearman correlation graph for both input and output variables.

2.4. Machine Learning (ML) Techniques

To obtain the desired results, machine-learning algorithms require a wide variety of input variables [8]. This study included the collection of 140 data samples from quarry mining operations, which were then used to train and test machine learning techniques. In this study, we were using MATLAB R2023a software to develop and analyse the machine learning models. The data were obtained by considering the proportions of the combinations and intended outcomes. This was undertaken because the models required comparable input variables for every combination to predict the desired outcome. Table 2 provides a concise summary of the statistical details of the variables.

Table 2. Descriptive statistics of the variables.

Variables	N	Missing	Mean	Median	SD	Variance	Range	Minimum	Maximum
n	140	0	78.729	70.00	46.746	2185.178	313	10	323
B/De	140	0	0.000	0.00	0.000	0.000	0	0	0
H/B	140	0	1.779	2.00	0.563	0.318	3.00	0.00	3.00
B	140	0	3.871	4.00	0.336	0.113	1	3	4
S	140	0	4.536	5.00	0.515	0.265	2	3	5
Q	140	0	0.707	0.00	1.837	3.374	12	0	12
SD	140	0	57.257	55.00	23.277	541.833	144	16	160
PPV	140	0	14.571	14.50	4.560	20.793	27	1	28

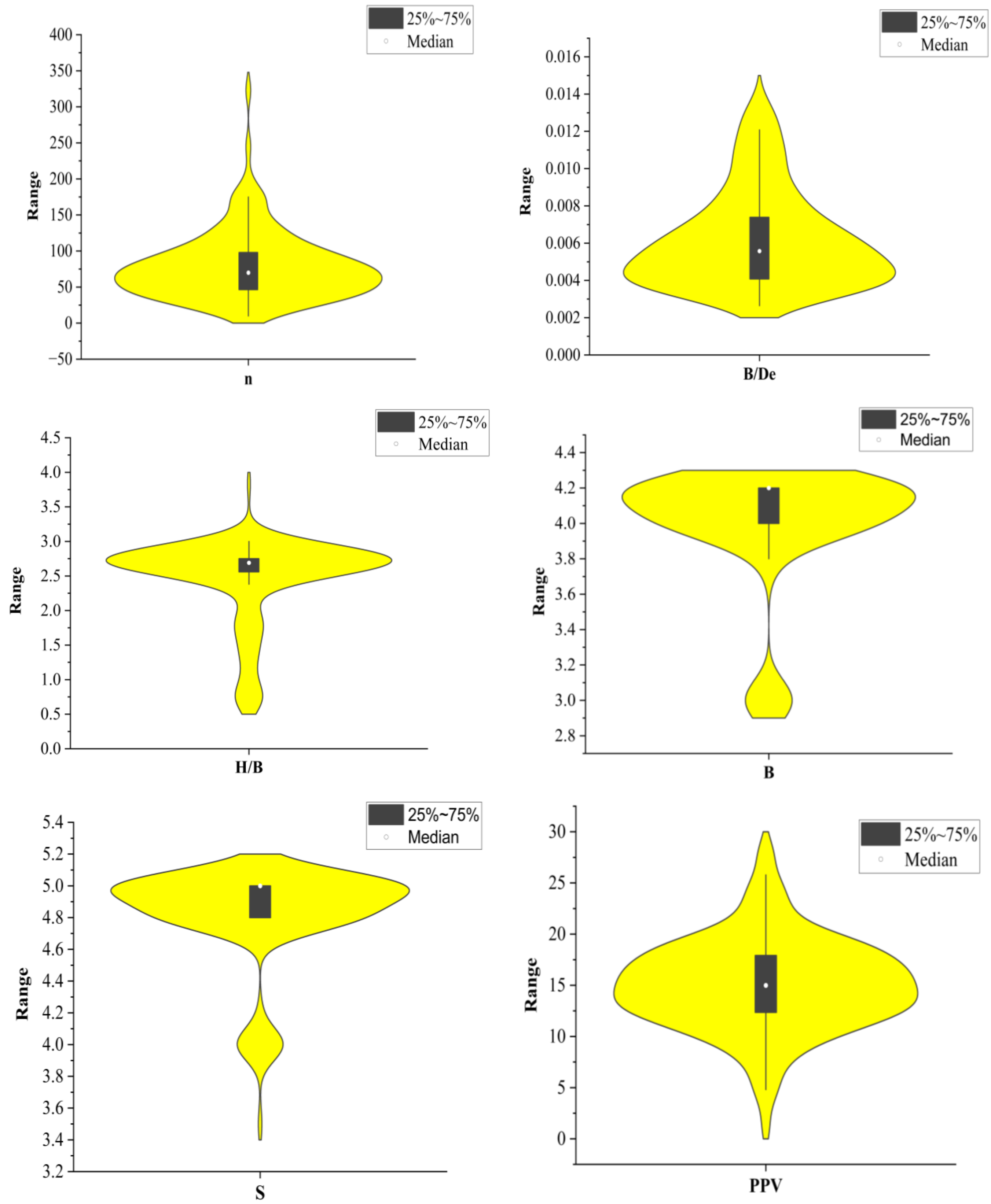

Figure 7. *Cont.*

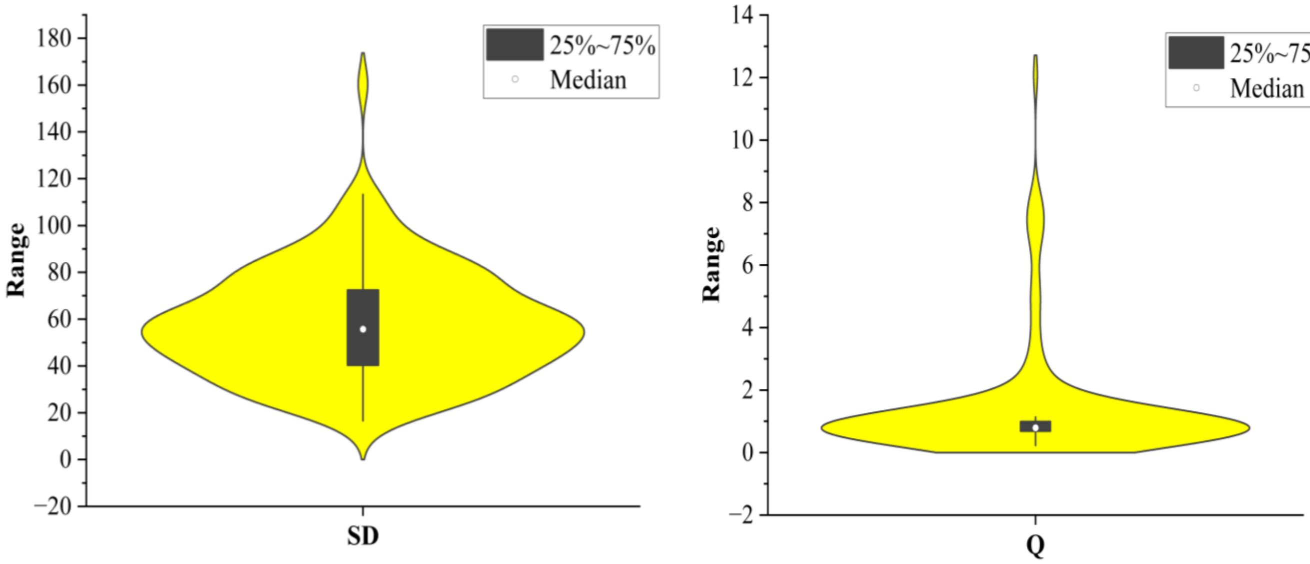

Figure 7. Violin plots for showing the input and output variables, both with median and quartiles at 25~75% (Q_1 and Q_3).

The model's testing and training data samples were allocated at a ratio of 20% and 80%, respectively. The measure of accuracy for a model may be determined by examining the R^2 value associated with the predicted outcome. The evaluation metrics approach and statistical measurements, such as MAE, RMSE, and MSE, were used to assess the accuracy of a model. The sequential arrangement of study techniques is shown in Figure 9. The dataset was split into the train (80%) and the test (20%) sets. Normalisation was applied to avoid overfitting and increase the model's learning performance. Equation (1) expresses the formula for normalisation. The next sections provide detailed explanations of the machine learning algorithms and validation methodologies used in this work.

$$x_{normalised} = \frac{(x - x_{minimum})}{(x_{maximum} - x_{minimum})} \quad (1)$$

where x represents the initial value, $x_{minimum}$ represents the minimum value in the dataset, $x_{maximum}$ represents the highest value in the dataset, and x normalised represents the normalised value. Normalisation is typically between 0 and 1.

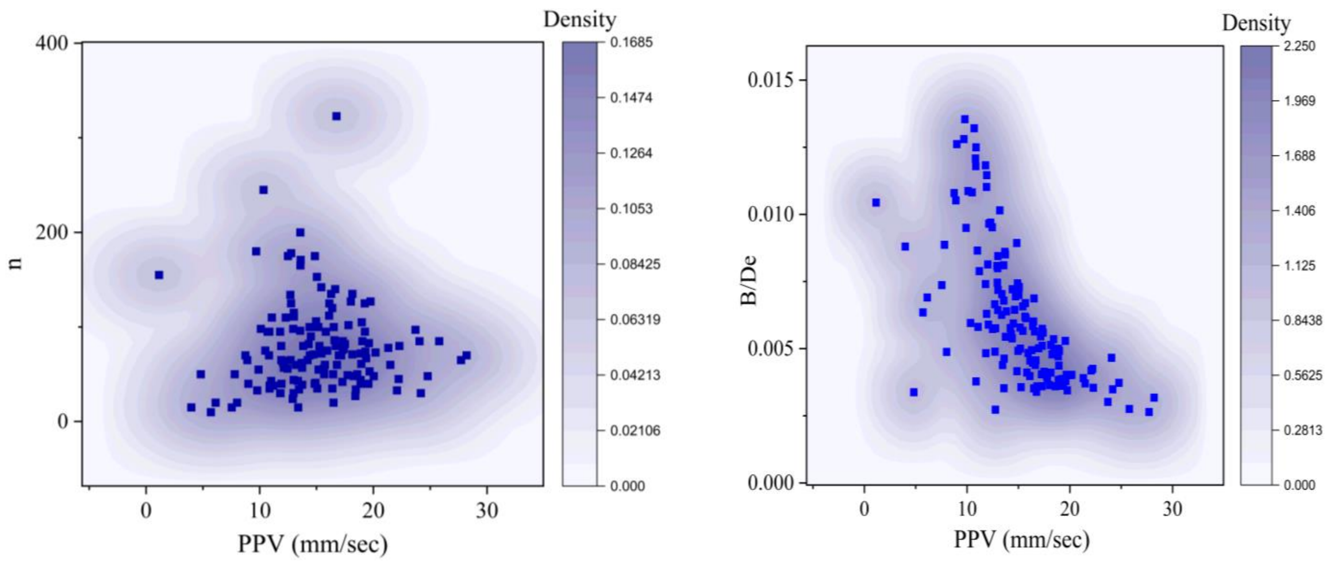

Figure 8. *Cont.*

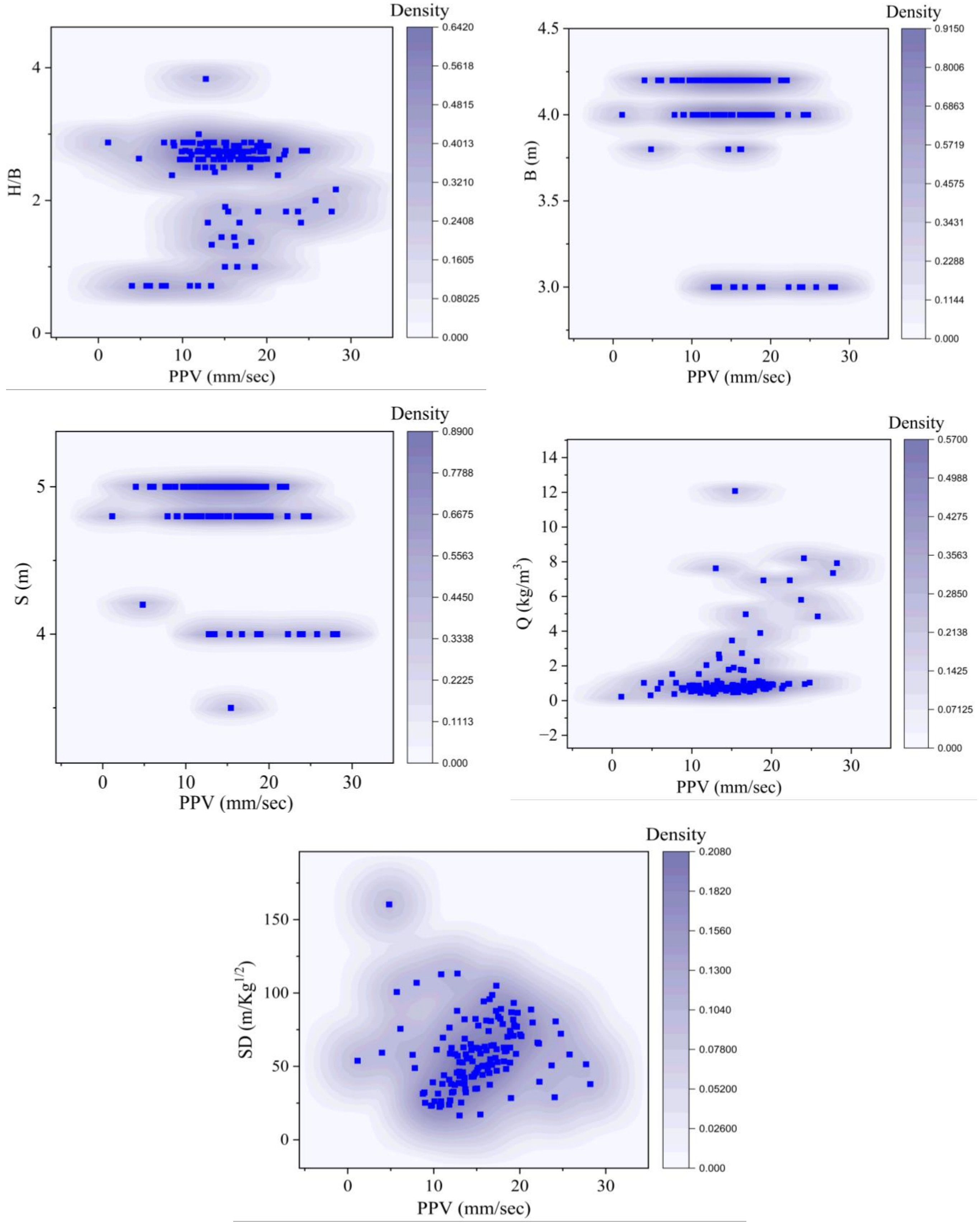

Figure 8. Two-dimensional kernel density estimation (KDE) to visualize each input variable with the output variable.

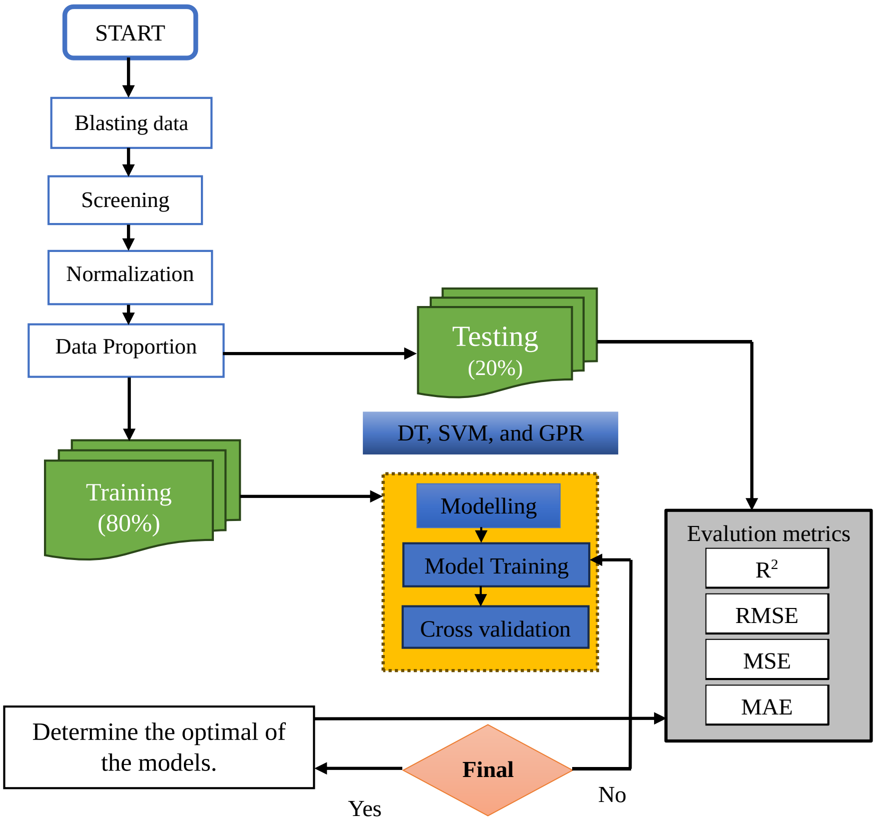

Figure 9. Flowchart of the study.

2.4.1. Decision Tree (DT)

According to Jitendra et al. [31], a decision tree is a graphical representation that resembles a flowchart, consisting of nodes, branches, and leaves. It is often used in the fields of operations research and operations management to solve problems. The flowchart depicts the hierarchical arrangement of categorisation rules, starting from the root and extending to the leaf nodes. The main components of the DT model are the chance nodes, decision nodes, and end nodes [32,33]. The DT optimizer configuration for this study is summarised in Table 3.

Table 3. DT optimizer configurations.

Main Parameters	Condition
Iteration	30
Maximum time for training	300 s
Number of grid division	10
Optimizer	Bayesian Optimisation
Acquisition function	Expected improved per second plus

Decision trees work well for blasting data because they are simple to grasp. They handle categorical and numerical data and are less susceptible to outliers. However, decision trees overfit small datasets, reducing their generalisability. They have difficulties capturing complicated correlations in the data and may need substantial filtering to avoid overfitting with insufficient data points.

2.4.2. Support Vector Machine (SVM)

Vladimir Vapnik introduced the SVM as a tool for analysing data in the context of regression analyses and classification issues. The SVM is under the domain of supervised machine learning. SVMs rely on the use of kernel functions, namely Gaussian, linear, quadratic, and cubic kernels [31]. The support vector machine (SVM) algorithm aims to minimise an upper limit on the generalisation error by maximising the margin between the hyperplane and the data points. This concept is shown in Figure 10.

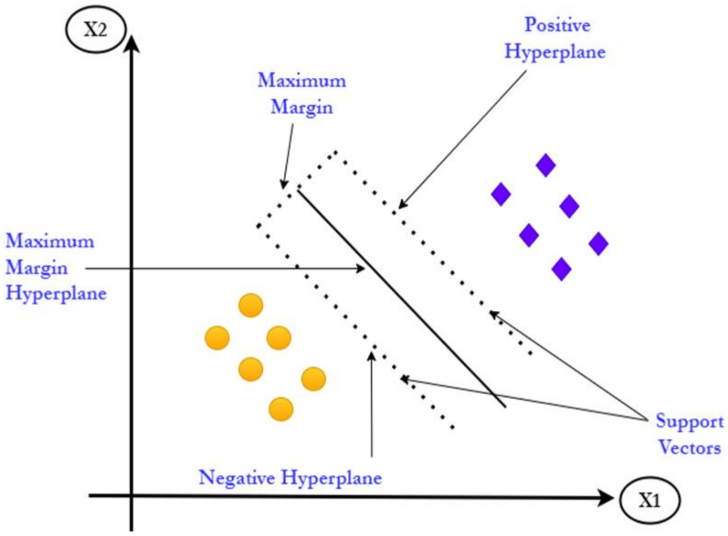

Figure 10. SVM formulation techniques.

SVMs minimise overfitting by maximising class margins in small datasets. Kernels may represent complicated non-linear relationships. Having too many characteristics relative to data points may make SVMs less effective. Determining a kernel function and hyperparameters is necessary but computationally demanding for small datasets.

2.4.3. Gaussian Process Regression (GPR)

The GPR is a probabilistic and Bayesian methodology model used for regression tasks within the domain of machine learning. One significant benefit of the GPR is its effectiveness in analysing limited datasets, exhibiting a high level of accuracy in its predictions.

From the research by Jitendra et al. [31] and Volker L et al. [34], a perspective GPR may be indicated as a nonlinear and nonparametric regression technique that proves to be valuable in the process of interpolating data points that are dispersed inside a high-dimensional input space. The GPR optimizer configuration for this study is summarised in Table 4. For limited datasets, the GPR gives predicted probabilities and uncertainty estimates, making it powerful. It adapts to limited observations and models complicated data connections.

Table 4. GPR hyperparameter configurations.

Main Parameters	Condition/Value
Kernel scale	Auto
Kernel function	Auto
Basic function	Auto
Sigma	Auto
Signal standard deviation	3.55
Optimizer numeric parameters	Enable
Standardize	Enable

3. Result and Discussion

3.1. DT Model

The findings of the DT model for evaluating the PPV are shown in Figure 11. Figure 11a illustrates the correlation between the measured and the predicted values (PPVs). The DT technique provided a reasonably accurate estimation of the positive predictive value, while there was some variation and discrepancy between the actual results and the anticipated values. The coefficient of determination (R^2) value of 0.73 indicates that the DT approach used to estimate the predictive value of ground vibrations is considered acceptable, and Figure 11b displays the distribution of the actual, estimated, and error values for the DT model. The error values exhibited a range of 0 to 0.98. Furthermore, an analysis was conducted to determine the percentage deviation of errors. The results revealed that 43% of the error measurements exhibited values below 0.05, while 57% fell in the range of 0.1 to 0.73. The examination of mistakes revealed that the DT method provided a reasonable estimation of the predictive value of the blasting technique.

(**a**)

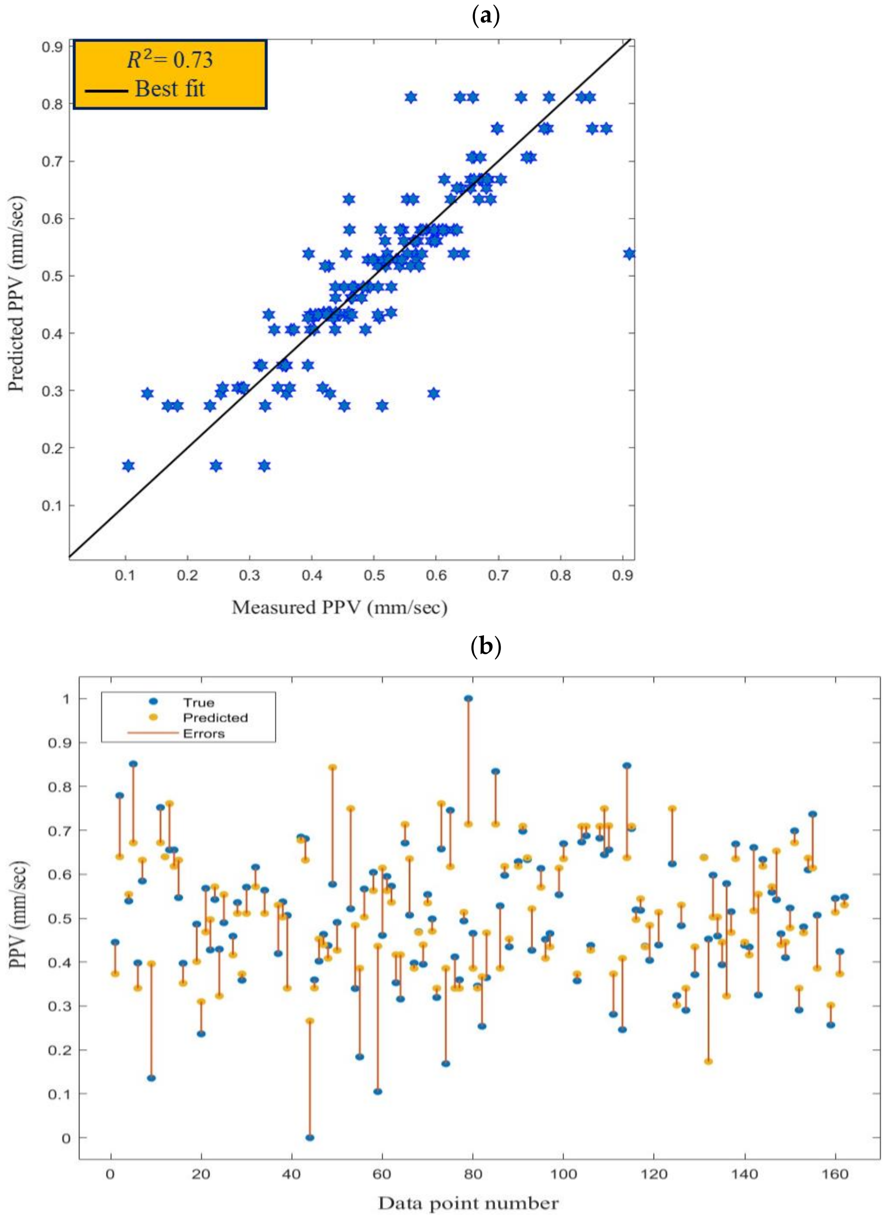

Figure 11. (**a**) Comparison between measured and predicted of the PPV using the decision tree model for the testing dataset. (**b**) Decision tree model performance plot of the variation in error between the measured and predicted values.

3.2. SVM Model

The results of the support vector machine (SVM) model in predicting the PPV are shown in Figure 12. The correlation between the observed and predicted positive predictive values (PPVs) is seen in Figure 12a. When comparing the DT and GPR approaches, it was seen that the SVM method yielded less accurate results, with a maximum difference observed between the actual and predicted findings and an R^2 value of 0.68. Based on the analysis of error deviations, it was determined that the SVR model exhibited comparatively lower accuracy in comparison to the DT and GPR models.

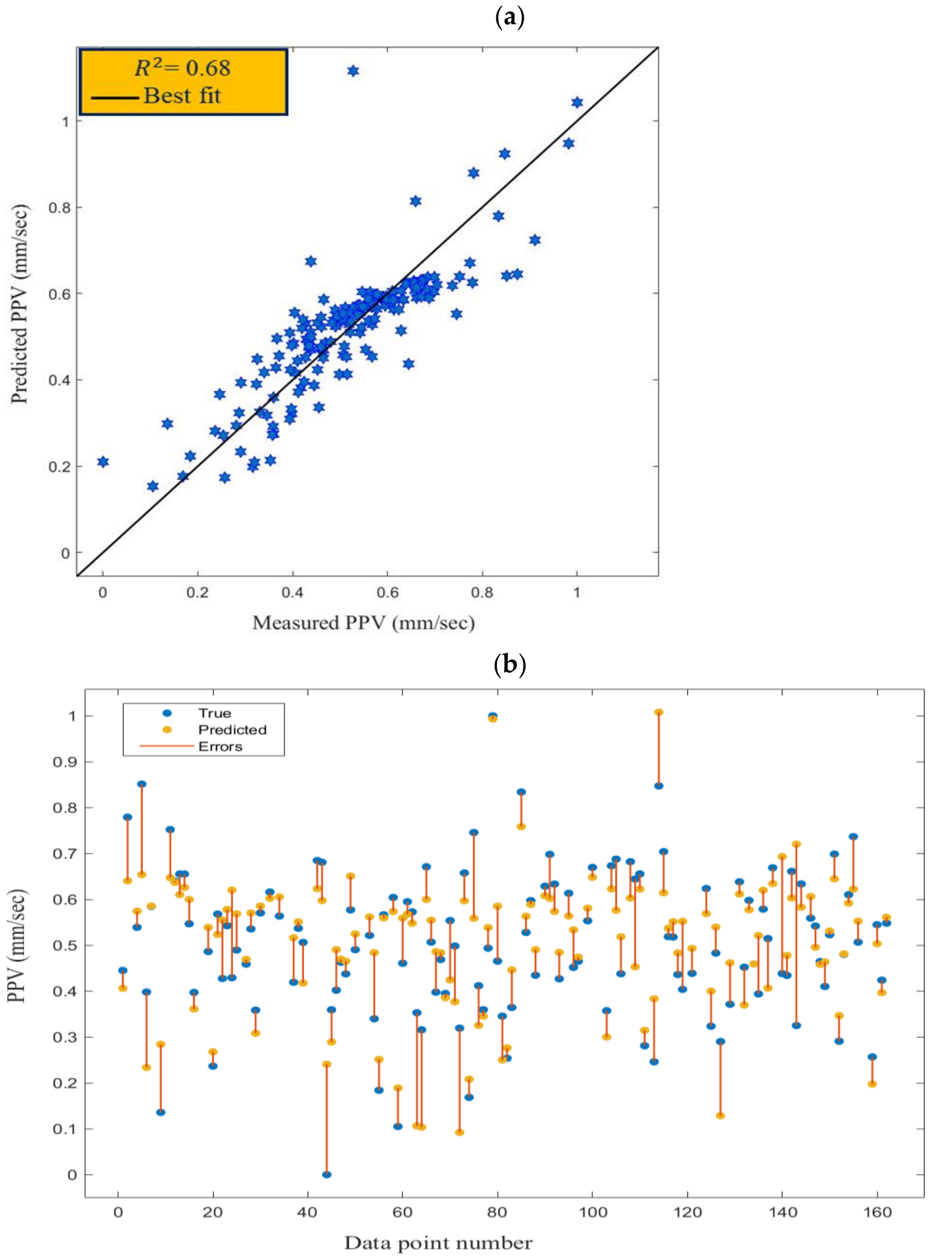

Figure 12. (**a**) Comparison between measured and predicted of the PPV using the spport vector machine model for the testing dataset. (**b**) SVM model performance plot of the variation in error between the measured and predicted values.

3.3. GPR Model

The GPR model has a higher level of precision in comparison to the other models, as seen by its R^2 score of 0.94. Figure 13b illustrates the distribution of true, estimated, and error values produced by the GPR technique. The findings of the GPR approach for predicting the PPV are shown in Figure 13. Figure 13a illustrates the relationship between the observed and predicted PPV. The RMSE was determined to be 0.038, the MSE was found to be 0.001, and the MAE was computed as 0.026. Most of the errors were determined to be below 0.02. The analysis of the error distribution revealed that the GPR model exhibited higher accuracy compared to the DT and SVM models. Therefore, this research demonstrates that the GPR model exhibits the best level of performance in accurately estimating the PPV, as seen by its producing lowest error observed in both the training and testing phases.

(**a**)

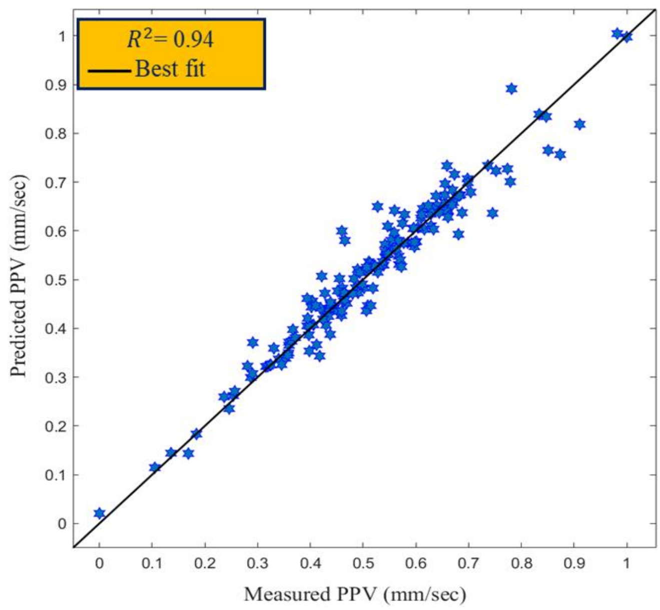

(**b**)

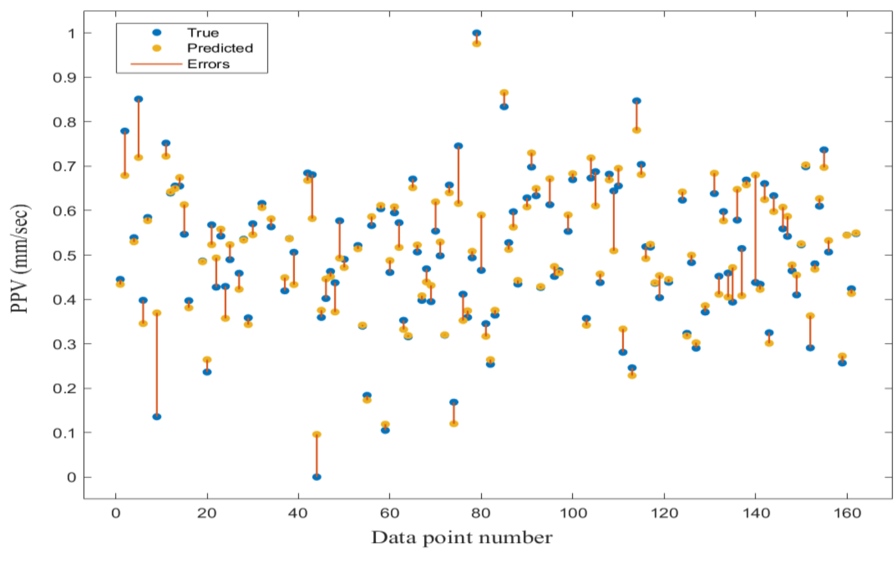

Figure 13. (**a**) Comparison between measured and predicted of the PPV using the Gaussin process regression model for the testing dataset. (**b**) GPR model performance plot of the variation in error between the measured and predicted values. The test results of each model are summarised in a tabular form, Table 5, and graph, Figure 14, and as for the training results, they are summarised in a tabular form, Table 6, and graphed in Figure 15.

Table 5. Evaluation metric results of each model in the testing.

Models	RMSE	MSE	MAE	R^2
DT	0.083	0.006	0.050	0.73
SVM	0.090	0.008	0.063	0.68
GPR	0.038	0.001	0.026	0.94

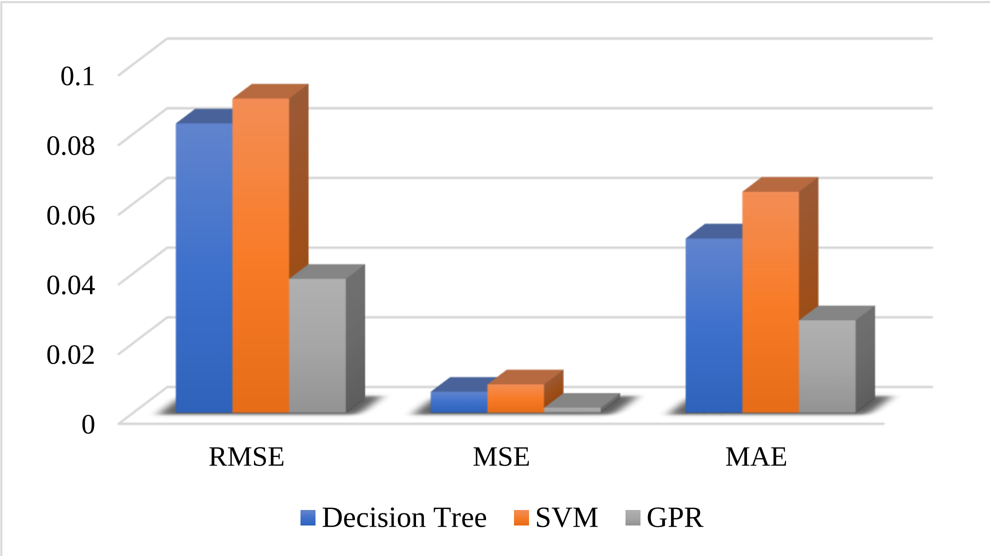

Figure 14. Test results of the three models based on their performance evaluation metrics.

Table 6. Evaluation metric result of each model in the training.

Models	RMSE	MSE	MAE	R^2
DT	0.010	0.006	0.074	0.58
SVM	0.009	0.008	0.071	0.64
GPR	0.002	0	0.035	0.89

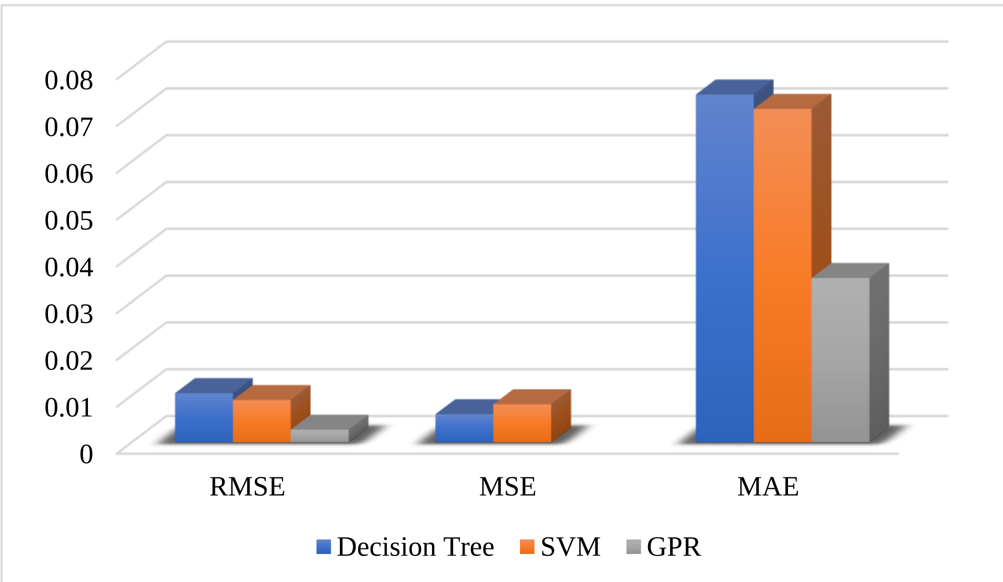

Figure 15. Training results of the three models based on their performance evaluation metrics.

3.4. Validation of the Models

The machine learning methods completed validation via the use of statistical tests and radar plot methodologies. Figure 16 depicts the connection between the three assessment metrics for each model in a triangular radar map. Notably, the model shown by a smaller triangle corresponds to the GPR. This implies that the model has a high level of accuracy. The performance of the ML approach is enhanced when the magnitude of errors is reduced and the R^2 coefficient is increased. Statistical measures, namely the mean absolute error (MAE), root mean square error (RMSE), and mean squared error (MSE), were used to evaluate the precision of each machine learning (ML) technique. The forecasts provided by the machine learning algorithms were subjected to a statistical analysis using Equations (2)–(5).

$$R^2 = 1 - \frac{\sum_i (PPV_i - PPV_i')^2}{\sum_i (PPV_i - \overline{PPV}_i)^2} \tag{2}$$

$$MSE = \frac{1}{N}\sum_{i=1}^{N}(PPV_i - PPV_i')^2 \tag{3}$$

$$RMSE = \sqrt{\frac{1}{n}\sum_{i=1}^{n}(PPV_i - PPV_i')^2} \tag{4}$$

$$MAE = \frac{1}{N}\sum_{i=1}^{N}|PPV_i - PPV_i'| \tag{5}$$

where N = the total number of blasting data points, PPV_i = predicted PPV, and PPV_i' = measured PPV.

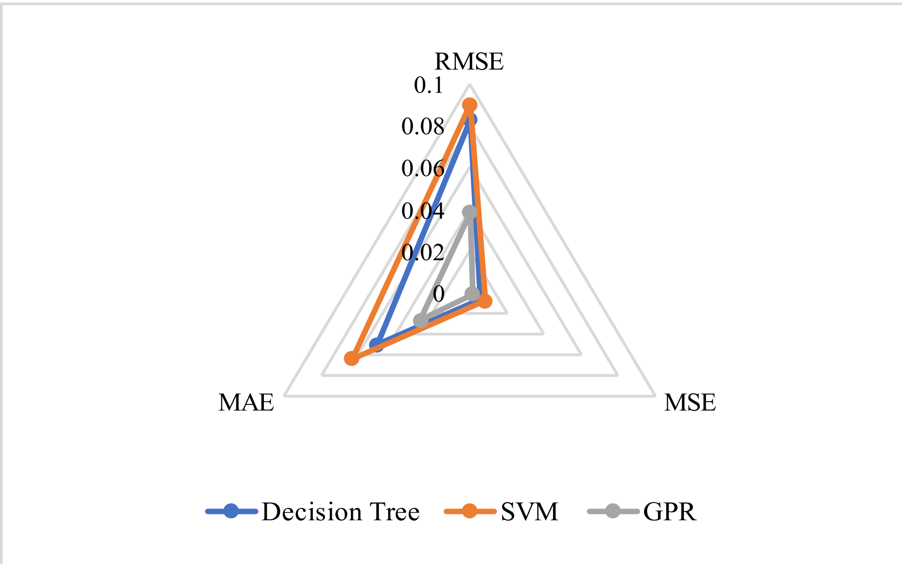

Figure 16. Radar plot for DT, SVM, and GPR models with their evaluation metric values.

3.5. Sensitivity Analysis

The input parameters were examined using a sensitivity analysis in this research. When an input variable changes, the prediction's sensitivity measures the change. An increased sensitivity indicates that the prediction is more sensitive to the input variable changes. Based on Figure 17, the most essential variables for predicting the PPV are B/De, H/B, and B (m), while the least important are S (m), Q (kg/m^3), and SD (m/kg$^{1/2}$). A low sensitivity implies that the prediction is least responsive to changes in these factors. Importantly, an input variable's sensitivity depends on the other input variables. The sensitivity of B/De may increase with increasing H/B levels. Overall, the sensitivity analysis image shows that the PPV prediction is most sensitive to changes in the B/De, H/B, and B (m) variables. These variables should be given the most attention when developing strategies for improving the PPV.

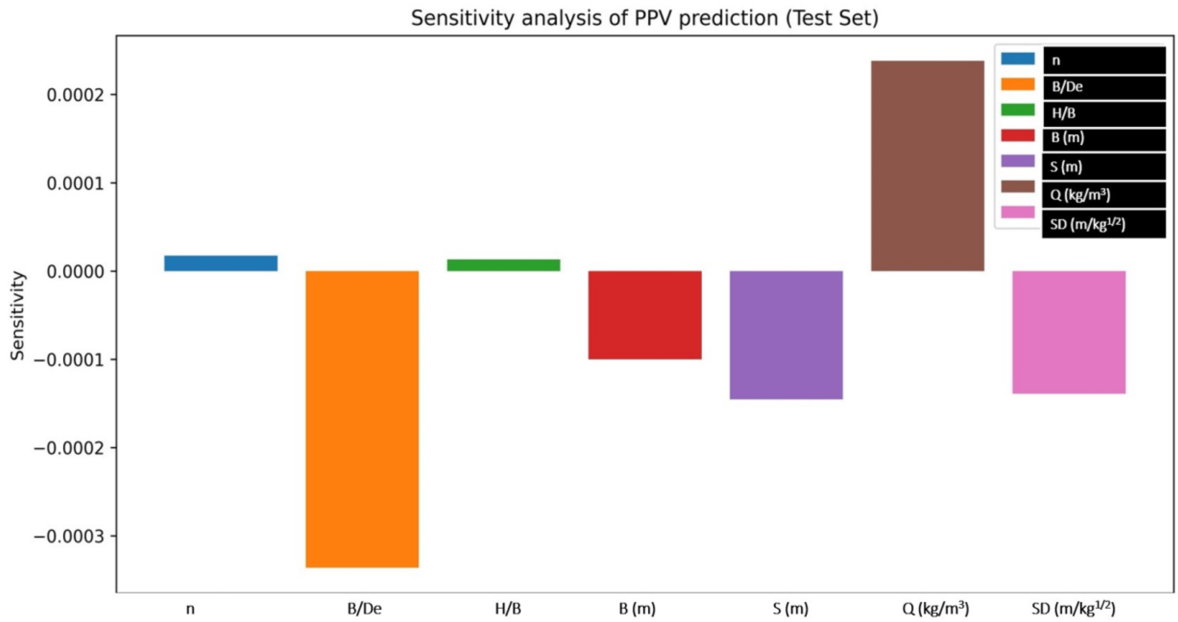

Figure 17. Sensitivity analysis of input parameters.

Here are some specific interpretations of the sensitivity analysis for each input variable:

- B/De: The ratio of the blast charge weight to the effective distance. A higher B/De ratio means that more energy is released closer to the target, which can lead to a higher PPV.
- H/B: The ratio of the hole depth to the blast charge diameter. A higher H/B ratio means that the blast charge is more deeply confined, which can also lead to a higher PPV.
- B (m): The blast charge diameter. A more significant blast charge diameter will generally result in a higher PPV.
- S (m): The spacing between blast holes. A smaller spacing will generally result in a higher PPV, but it is essential to consider other factors, such as safety and ground vibration, when selecting the spacing.
- Q (kg/m^3): The rock density. A higher rock density will generally result in a higher PPV.
- SD (m/kg$^{1/2}$): The specific drill energy. This measures the energy required to drill a unit volume of rock. A higher specific drill energy will generally result in a lower PPV.

3.6. Shapley Additive Explanation (SHAP)

The Shapley additive explanation (SHAP) framework is an essential tool used for the interpretation of results generated by machine learning algorithms. The framework assigns a numerical weight to each feature, which serves to further explain the model's output and clarify the influence of every feature on the predicted outcome (refer to Figure 18). Shapley values provide a fair distribution of the total worth of a cooperative game by considering the specific contributions made by each player towards the game's outcome. Within the realm of machine learning, SHAP values use an approach that is analogous in nature to allocating the contribution of each feature towards the output of the model [30]. In this study, Figure 18a depicts the trend and distribution of the SHAP values attributed to each input variable. The y-axis represents the input variables, arranged in a descending order of importance, while the x-axis illustrates the corresponding SHAP values, and Figure 18b provides an individual interpretation for every input variable n, B/De, SD, H/B, and Q.

(**a**)

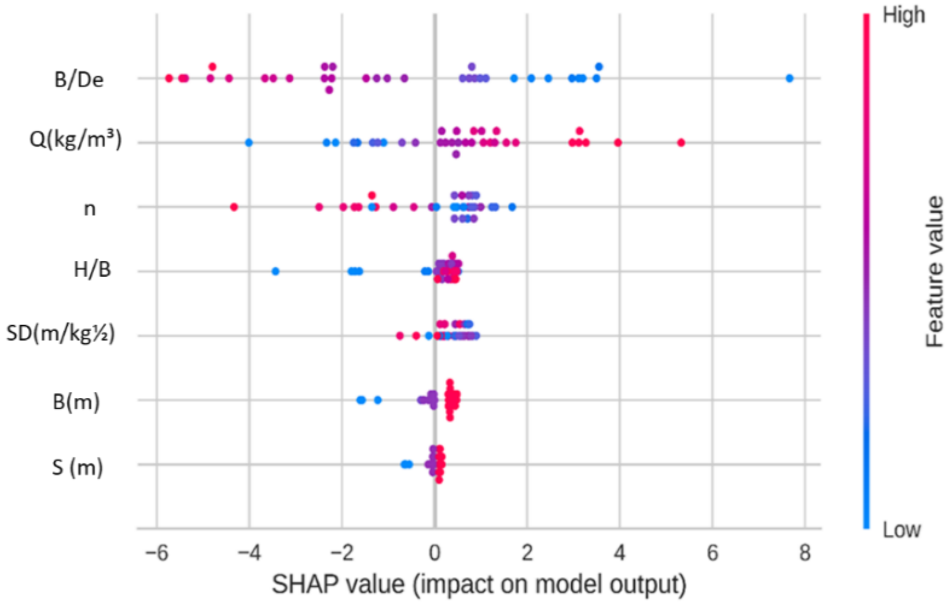

(**b**)

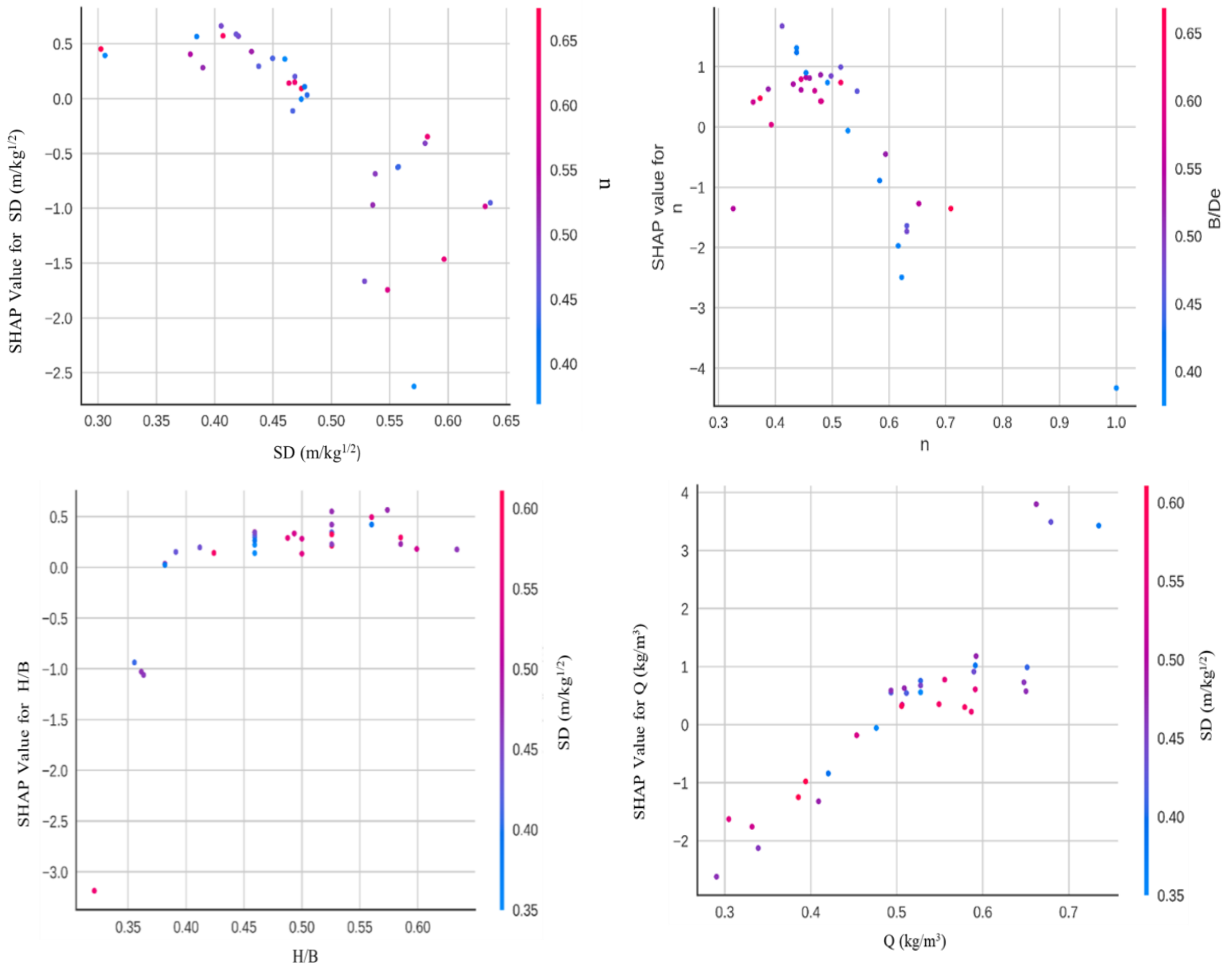

Figure 18. (**a**) Distribution of the SHAP values attributed to each input variables, (**b**) provides an individual interpretation for every input variable n, B/De, SD, H/B, and Q.

4. Conclusions

The objective of this study is to predict the blast-induced ground vibration of a dolomite quarry using three soft computing techniques and four statistical evaluation metrics. The following statements include many deductions that may be inferred from the research that was given.

The proposed model for this study was built using a set of seven input parameters (N, B/De, B, S, Q, SD, H/B) and a dataset including 140 recorded instances of blasting. The dataset is partitioned into two distinct proportions: the training data, which constitutes 80% of the overall dataset, and the test data, which accounts for the remaining 20% of the total dataset.

The comparative evaluation of two models was conducted using several performance evaluation measures, including the mean squared error (MSE), the root-mean-square error (RMSE), and Pearson's correlation coefficient (R^2). Furthermore, a potential Shapley additive explanation (SHAP) technique was used after the model assessment to obtain insights into the significance of individual features in the model.

The results found from the GPR model are compared with the two machine learning regression analyses (i.e., DT and SVM), and we found that the performances of the GPR model are superior to those of the other two models, with a lower error (RMSE = 0.038, MSE = 0.001, MAE = 0.026, and R^2 = 0.94).

In consideration of the number of factors and the assessment criteria, these findings can be regarded as remarkably accurate. For the estimation of the PPV parameters, two machine learning algorithms were evaluated. The findings indicated that these relationships have weak PPV estimation capabilities. Due to its nonlinear structure, great flexibility, and low error, a GPR is much more capable of estimating the PPV than the other models.

This study has twofold significance. The present study aims to fill a notable need in existing research by integrating robust machine learning techniques, namely GPRs in the investigation of ground vibrations resulting from explosive occurrences.

Adopting a GPR as a soft computing approach and optimising the GPR model may allow us to predict the PPV before an explosion. The optimisation model may be used to adjust the blast design to eliminate blast disturbances such as fly rock, ground vibrations, air blasts, etc., and maximise explosive energy use. Using a GPR to simulate and predict blasting-induced ground vibrations is the study's main contribution. The GPR can capture complicated, non-linear correlations in data, making it ideal for blast-induced ground vibrations, which are dynamic and nonlinear.

This study does not optimise the GPR, but it is suggested for further research. With short datasets, decision trees, support vector machines, and Gaussian process regression may overfit, resulting in models that may not generalise effectively. They may not capture complex relationships in the data, which could be a limitation when dealing with blast-induced ground vibrations. SVMs can perform well with small datasets, but finding a suitable kernel and parameter tuning can be difficult.

Author Contributions: Conceptualisation, Y.F.; methodology, Y.F.; software, Y.F.; validation, Y.F.; formal analysis, Y.F.; investigation, Y.F.; resources, H.I. and T.A.; data curation, H.I. and N.O.; writing—original draft preparation, Y.F.; writing—review and editing, Y.F.; visualisation, Y.K. and T.A.; supervision, H.T. and T.A.; project administration, Y.K. and N.O.; funding acquisition, Y.K. and H.I. All authors have read and agreed to the published version of the manuscript.

Funding: This research received no external funding.

Institutional Review Board Statement: Not applicable.

Informed Consent Statement: Not applicable.

Data Availability Statement: The data will be available on request from the corresponding author.

Acknowledgments: We thank Engineer Taiwo for his constant support and cooperation in this research.

Conflicts of Interest: The authors declare no conflict of interest.

Abbreviations

AI	Artificial intelligence
ANN	Artificial neural network
ANFS	Adaptive neuro fuzzy model
B	Burden
B/De	Burden-to-diameter ratio
B/S	Burden-to-spacing ratio
CPH	Charge per hole
D	Distance
Dh	Horizontal distance
E	Young's modulus
ED	Elevation difference
GA	Genetic algorithm
GEP	Gene expression programming
GPR	Gaussian process regression
HD	Hole depth
HDM	Hole diameter
H/B	Stiffness ratio
HD/B	Hole depth-to-burden ratio
IC	Integrity coefficient
ICA	Imperialist competitive algorithm
MAE	Mean absolute error
MAPE	Mean absolute error percentage
MARS	Multivariate adaptive regression splines
MCPD	Maximum charge per delay
MLR	Multiple linear regression
MSE	Mean-squared error
MVRA	Multivariate regression analysis
N	Number of holes
NLMR	Nonlinear multiple regression
PF	Powder factor
Pv	P-wave
PPR	Presplit penetration ratio
PPV	Peak particle velocity
PSO	Particle swarm optimization
Qmax	Maximum charge per delay
Qtoat	Total amount of charge
R^2	Coefficient of determination
RMSE	Root-mean-square error
RQD	Rock quality designation
S	Spacing
SHAP	Shapley additive explanation
SL	Stemming length
SVR	Support vector regression
T	Stemming
TC	Total charge
TS	Tunnel cross section
VAF	Variance accounted for
VoD	Velocity of detonator
XGBoost	Extreme gradient-boosting
Ve	Volume of extracted block

References

1. Fissha, Y.; Ikeda, H.; Toriya, H.; Adachi, T.; Kawamura, Y. Application of Bayesian Neural Network (BNN) for the Prediction of Blast-Induced Ground Vibration. *Appl. Sci.* **2023**, *13*, 3128. [CrossRef]
2. Fissha, Y. Mining for a Sustainable World: The Adoption of Sustainable Blasting Techniques. *Asp. Min. Miner. Sci.* **2023**, *10*, 1175–1176. [CrossRef]

3. Yewuhalashet, B.O.T.F. Quarry Slope Stability Assessment Methods with Blast Induced Effect Monitoring in Akoko Edo, Nigeria. *Geotech. Geol. Eng.* **2023**, *41*, 2553–2571. [CrossRef]
4. Taiwo, B.O.; Yewuhalashet, F.; Adamolekun, L.B.; Bidemi, O.O.; Famobuwa, O.V.; Victoria, A.O. Development of Artificial Neural Network Based Mathematical Models for Predicting Small Scale Quarry Powder Factor for Efficient Fragmentation Coupled with Uniformity Index Model. *Artif. Intell. Rev.* **2023**, *56*, 14535–14556. [CrossRef]
5. Olamide Taiwo, B. Improvement of Small-Scale Dolomite Blasting Productivity: Comparison of Existing Empirical Models with Image Analysis Software and Artificial Neural Network Models. *J. Min. Environ.* **2022**, *13*, 627–641. [CrossRef]
6. Kweku, C.; Victor, A.; Temeng, A.; Yevenyo, Y. Novel Approach to Predicting Blast-Induced Ground Vibration Using Gaussian Process Regression. *Eng. Comput.* **2020**, *36*, 29–42. [CrossRef]
7. Onederra, I.A.; Furtney, J.K.; Sellers, E.; Iverson, S. International Journal of Rock Mechanics & Mining Sciences Modelling Blast Induced Damage from a Fully Coupled Explosive Charge. *Int. J. Rock Mech. Min. Sci.* **2013**, *58*, 73–84. [CrossRef]
8. Ragam, P.; Komalla, A.R.; Kanne, N. Estimation of Blast-Induced Peak Particle Velocity Using Ensemble Machine Estimation of Blast-Induced Peak Particle Velocity Using Ensemble Machine Learning Algorithms: A Case Study. *Noise Vib. Worldw.* **2022**, *53*, 404–413. [CrossRef]
9. Khandelwal, M.; Jahed, D.; Roohollah, A.; Faradonbeh, S. Classification and Regression Tree Technique in Estimating Peak Particle Velocity Caused by Blasting. *Eng. Comput.* **2017**, *33*, 45–53. [CrossRef]
10. Khandelwal, M.; Kankar, P.K. Prediction of Blast-Induced Air Overpressure Using Support Vector Machine. *Arab. J. Geosci.* **2011**, *4*, 427–433. [CrossRef]
11. Zhou, J.; Li, C.; Koopialipoor, M.; Armaghani, D.J.; Pham, B.T. Development of a New Methodology for Estimating the Amount of PPV in Surface Mines Based on Prediction and Probabilistic Models (GEP-MC). *Int. J. Min. Reclam. Environ.* **2020**, *35*, 48–68. [CrossRef]
12. Khandelwal, M.; Kumar, D.L.; Yellishetty, M. Application of Soft Computing to Predict Blast-Induced Ground Vibration. *Eng. Comput.* **2011**, *27*, 117–125. [CrossRef]
13. Kumar, A.; Singh, P.; Sharma, S.K.; Kishore, N.; Singh, C.S. Quantitative Assessment of BIGV and Structural Response Based on Velocity and Frequency around an Opencast Mine. *Curr. Sci.* **2021**, *121*, 275–285. [CrossRef]
14. Kekeç, B.; Ghiloufi, D. Propagation characteristics of surface and in-depth vibrations in sand grounds: A comparative analysis. *Konya J. Eng. Sci.* **2022**, *10*, 1–17. [CrossRef]
15. Paurush, P.; Rai, P.; Sharma, S.K. Selection of Blasting Design Parameters Affecting Peak Particle Velocity—A Case Study. *Min. Metall. Explor.* **2021**, *38*, 1435–1447. [CrossRef]
16. Görgülü, K.; Arpaz, E.; Demirci, A.; Koçaslan, A.; Dilmaç, M.K.; Yüksek, A.G. Investigation of Blast-Induced Ground Vibrations in the Tülü Boron Open Pit Mine. *Bull. Eng. Geol. Environ.* **2013**, *72*, 555–564. [CrossRef]
17. Saadat, M.; Khandelwal, M.; Monjezi, M. An ANN-Based Approach to Predict Blast-Induced Ground Vibration of Gol-E-Gohar Iron Ore Mine, Iran. *J. Rock Mech. Geotech. Eng.* **2014**, *6*, 67–76. [CrossRef]
18. Lawal, A.I.; Idris, M.A. An Artificial Neural Network-Based Mathematical Model for the Prediction of Blast-Induced Ground Vibrations. *Int. J. Environ. Stud.* **2020**, *77*, 318–334. [CrossRef]
19. Jahed Armaghani, D.; Hajihassani, M.; Monjezi, M.; Mohamad, E.T.; Marto, A.; Moghaddam, M.R. Application of Two Intelligent Systems in Predicting Environmental Impacts of Quarry Blasting. *Arab. J. Geosci.* **2015**, *8*, 9647–9665. [CrossRef]
20. Vasović, D.; Kostić, S.; Ravilić, M.; Trajković, S. Environmental Impact of Blasting at Drenovac Limestone Quarry (Serbia). *Environ. Earth Sci.* **2014**, *72*, 3915–3928. [CrossRef]
21. Khandelwal, M.; Singh, T.N. Evaluation of Blast-Induced Ground Vibration Predictors. *Soil Dyn. Earthq. Eng.* **2007**, *27*, 116–125. [CrossRef]
22. Nguyen, H.; Bui, X.-N.; Bui, H.-B.; Cuong, D.T. Developing an XGBoost model to predict blast-induced peak particle velocity in an open-pit mine: A case study. *Acta Geophys.* **2019**, *67*, 477–490. [CrossRef]
23. Lawal, A.I. An Artificial Neural Network-Based Mathematical Model for the Prediction of Blast-Induced Ground Vibration in Granite Quarries in Ibadan, Oyo State, Nigeria. *Sci. Afr.* **2020**, *8*, e00413. [CrossRef]
24. Zhang, Y. Study on Attenuation Law of Open-Pit Bench Blasting Vibration. *Procedia Eng.* **2014**, *84*, 868–872. [CrossRef]
25. Rana, A.; Bhagat, N.K.; Jadaun, G.P.; Rukhaiyar, S.; Pain, A.; Singh, P.K. Predicting Blast-Induced Ground Vibrations in Some Indian Tunnels: A Comparison of Decision Tree, Artificial Neural Network and Multivariate Regression Methods. *Min. Metall. Explor.* **2020**, *37*, 1039–1053. [CrossRef]
26. Verma, A.K.; Singh, T.N. Intelligent Systems for Ground Vibration Measurement: A Comparative Study. *Eng. Comput.* **2011**, *27*, 225–233. [CrossRef]
27. Ghasemi, E.; Ataei, M. Development of a Fuzzy Model for Predicting Ground Vibration Caused by Rock Blasting in Surface Mining. *J. Vib. Control* **2012**, *19*, 755–770. [CrossRef]
28. Iphar, M.; Yavuz, M.; Ak, H. Prediction of Ground Vibrations Resulting from the Blasting Operations in an Open-Pit Mine by Adaptive Neuro-Fuzzy Inference System. *Environ. Geol.* **2008**, *56*, 97–107. [CrossRef]
29. Xi, B.; Li, E.; Fissha, Y.; Zhou, J.; Segarra, P. LGBM-Based Modeling Scenarios to Compressive Strength of Recycled Aggregate Concrete with SHAP Analysis. *Mech. Adv. Mater. Struct.* **2023**. [CrossRef]
30. Hauke, J.; Kossowski, T. Comparison of Values of Pearson's and Spearman's Correlation Coefficients on the Same Sets of Data. *Quaest. Geogr.* **2011**, *30*, 87–93. [CrossRef]

31. Khatti, J.; Grover, K.S. Determination of the Optimum Performance Ai Model and Methodology To Predict the Compaction Parameters of Soils. *ICTACT J. Soft Comput.* **2022**, *12*, 2640–2650.
32. Kingsford, C.; Salzberg, S.L. What Are Decision Trees? *Nat. Biotechnol.* **2008**, *26*, 1011–1012. [CrossRef] [PubMed]
33. Kamiński, B.; Jakubczyk, M.; Szufel, P. A Framework for Sensitivity Analysis of Decision Trees. *Cent. Eur. J. Oper. Res.* **2018**, *26*, 135–159. [CrossRef] [PubMed]
34. Deringer, V.L.; Bartók, A.P.; Bernstein, N.; Wilkins, D.M.; Ceriotti, M.; Csányi, G. Gaussian Process Regression for Materials and Molecules. *Chem. Rev.* **2021**, *121*, 10073–10141. [CrossRef] [PubMed]